Leakage Currents in Illuminated Junctions and Biased Transistors

1. Summary

Analysis of the frequency dependence of the junction photo-voltage (JPV) in illuminated junctions (under weak forward bias) yields the amplitude of the ideal diode I-V characteristic, Io, dominated by the carrier recombination effects in the depletion layer. This carrier recombination leakage is strongly dependent on process conditions, which determine the dopant activation and profile shape, junction location and residual damage distribution in the junction.

Leakage in reverse biased transistors and diodes includes the effects of carrier generation, related to residual damage density and location relative to the junction boundary, as well as structure and bias dependent effects of gate oxide leakage, band-to-band tunneling at the drain junction and thermionic emission from metal contacts. All of these effects depend on process conditions, through dependence on dopant activation and profile shape, junction location and local electric fields. However, only the generation/recombination current is strongly sensitive to the residual defect density and location relative to the junction boundaries, which are strongly dependent on implant and annealing process conditions.

Comparisons of the dependence on process-sensitive effects (related to doping and damage distributions) for leakage currents measured in forward (RsL) and reverse (diodes & transistors) bias show that RsL measures have a much wider dynamic range than diode and transistor measurements, which are limited by effects of structural, contact and additional leakage factors, such as gate oxide conduction.

2. Sources of leakage currents in p-n junctions and transistors

The p-n junction (for example, a p^+ top junction with n^+ sub-junction doping) leakage current under reverse bias includes the contributions of diffusion current, J_{diff}, space charge generation current, J_{gen}, band-to-band tunneling current, J_{tun}, and thermionic emission current, J_{them}, [1]:

$$J_{leak} = J_{diff} + J_{gen} + J_{tun} + J_{therm} \ . \qquad (1)$$

Additional terms for MOS transistors include leakage from gate oxide conductance, as sketched in Fig. 1.

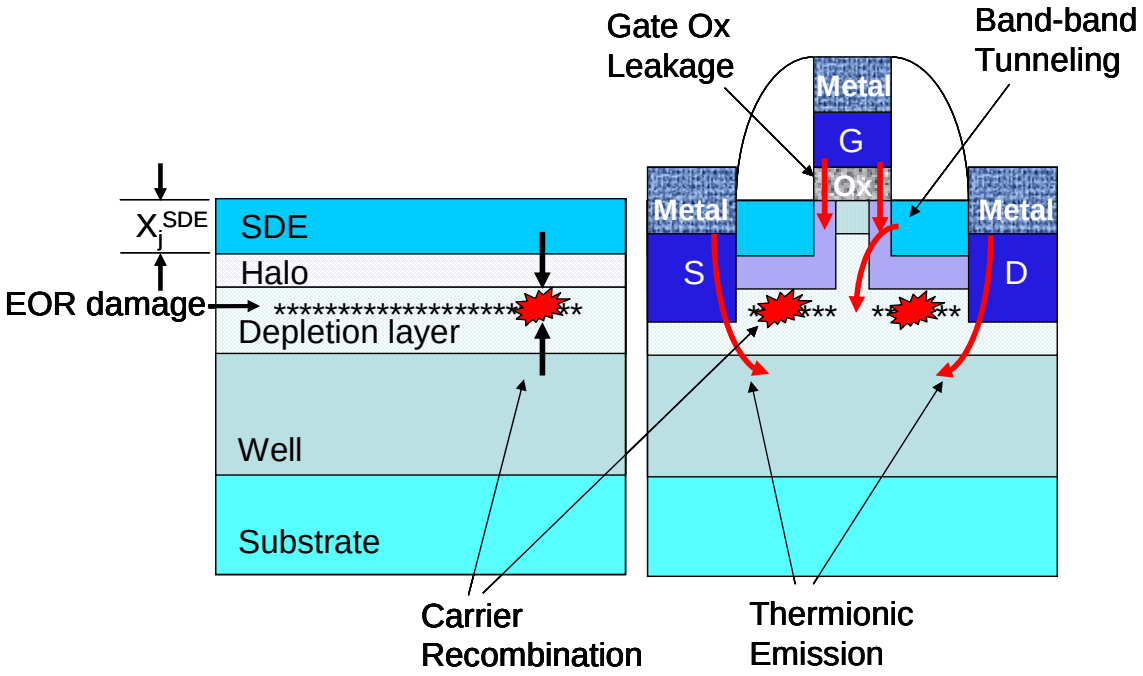

Figure 1. Sketch of leakage mechanisms in p-n junctions and transistors.

Carrier recombination/generation

Carrier recombination leakage, observed under forward bias, is determined primarily by the sub-junction doping density (which determines the width of the depletion layer) and the density and location of the residual damage after annealing from the accumulated damage due to the various implantation cycles. Damage accumulation during implantation depends on the ion type, target (usually Si), ion energy and dose as well as process specifics such as the ion beam current and wafer temperature during implantation. Under reverse bias conditions, defect centers are sources of carrier generation, with similar amplitude to the recombination rate. The generation current is described by:

$$J_{gen} = \sigma \cdot v_{th} n_i N \frac{qW}{2} = \sigma \cdot v_{th} n_i N_t \sqrt{\frac{q\varepsilon_S \varepsilon_0 (Na + Nd)(V_{bi} - V_{rb})}{2 N_A N_D}} \qquad (2)$$

where N_t, σ are the concentration of recombination centers and their capture cross section in a depletion region of p-n junction, W is depletion width, v_{th} is thermal velocity of carriers, q is the charge of the electron, ε_0 is permittivity of vacuum, ε_S is dielectric constant of silicon, N_a, N_d are doping in top and bottom layers of p-n junction, n_i is intrinsic concentration of carriers in silicon, V_{bi} is build in voltage of p-n junction, , V_{rb} is applied reverse bias [2].

The key features of generation/recombination current is that it is (1) dependent on the number of generation/recombination centers, usually identified with lattice imperfections such as end-of-range (EOR) dislocation layers and various forms of metal and oxygen precipitates and (2) dependent on the sub-junction doping, where the depletion layer decreases in thickness with increasing sub-junction doping. The most effective contributions to generation and recombination currents occur when the defect centers are located in the middle of the depletion layer, where the populations of carrier types available for recombination are close to equal. The principle process-sensitive parameters are (1) the location and density of residual implant damage, (2) surface junction depth and profile shape and (3) active sub-junction doping density.

The rate of carrier recombination, U(z), in the depleted layer is given by the Shockley-Read-Hall equation:

$$U(z) = \frac{\sigma_n \sigma_p v_{th} N_t(z) n_i \left[\exp\left(\frac{qV}{kT}\right) - 1 \right]}{\sigma_n \left[\exp\left(q\frac{\psi - \varphi_n}{kT} \right) + \exp\left(\frac{E_t - E_i}{kT} \right) \right] + \sigma_p \left[\exp\left(q\frac{\varphi_p - \psi}{kT} \right) + \exp\left(q\frac{E_i - E_t}{kT} \right) \right]} \quad (3)$$

where and V is the JPV, ψ=-Ei/q is the internal potential corresponding to the intrinsic level, Ei, φ_n , φ_p are the potentials corresponding to quasi-Fermi levels for electrons and holes, v_{th}, σ_n ,σ_p are thermal velocity and the capture cross sections of electrons and holes, Et, N_t is the energy level and concentration of recombination centers, n_i is intrinsic carrier concentration.

The leakage current is the integral of the recombination rate over the thickness of the depletion layer:

$$J_{rec} = \int_0^W qU(z)dz \quad (4)$$

The recombination profile and leakage current, I_o, can be calculated for low photo-voltage V=φ_n - φ_p << kT/q for an abrupt p-n junction, for the example with a junction depth, X_j = 100 A, with the residual damage profile described by:

$$N_t(z) = N_{t\max} \exp\left[-\frac{(z - z_{\max})^2}{\Delta^2} \right] + N_{tsub} \quad (5)$$

where the peak concentration of recombination sites N_{tmax}= 10^{18} traps/cm^3 at a depth of z_{max}= 200 A, with a trap profile width of Δ = 150 A, $\boldsymbol{\sigma_n}$,$\boldsymbol{\sigma_p}$ = 10^{-14} cm^2 , E_t=E_i, and N_{tsub}= 10^{12} traps/cm^3 is the concentration of recombination centers in the substrate, much deeper

than z_{max}. These parameters are descriptive of conditions for a shallow junction formed in an implanted halo profile. The recombination rate profiles, U(z), for substrate doping of 10^{15}, 10^{17} and 10^{19} dopants/cm^3 are shown in Fig. 2. And the integral leakage currents for three damage density values are shown in Fig. 3 [3].

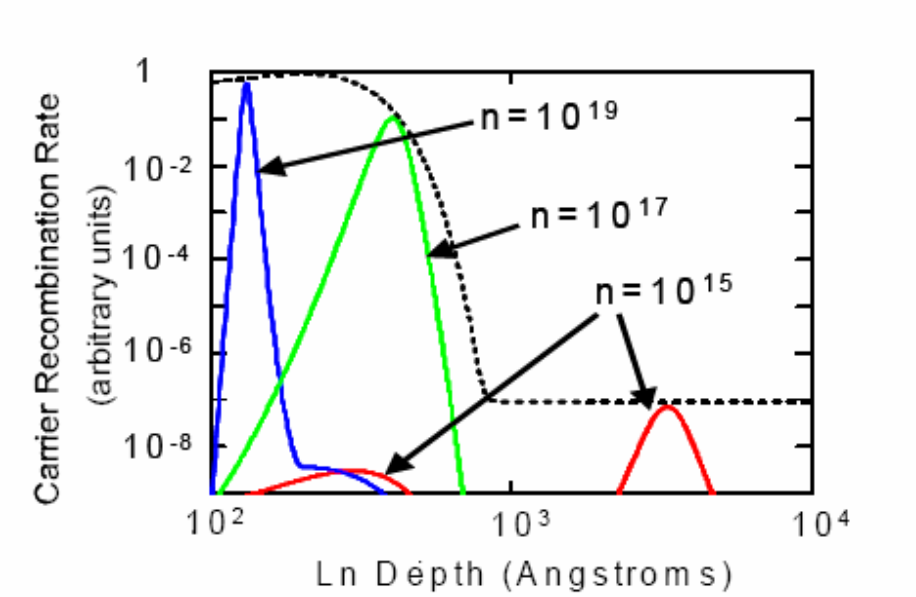

Figure 2. Recombination rate profiles below a shallow junction (Xj = 100 A) for a model end-of-range damage profile (dotted line) and substrate doping levels of 10^{15}, 10^{17} and 10^{19} dopants/cm^3.

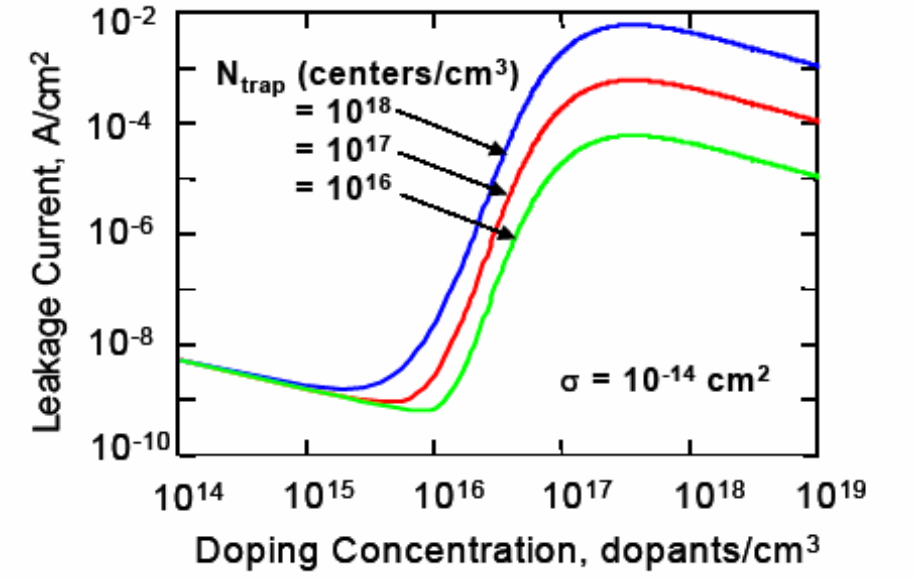

Figure 3. Leakage currents as a function of substrate doping for three trap densities.

Note that, according to the integral of Eq. 4, shown in Fig. 3, for lightly-doped substrates, with n ~ 10^{15} dopants/cm^3, the recombination leakage current is low and does not depend strongly on the density of recombination centers. For doping levels characteristic of shallow junctions in halo/well profiles, with n ~ 5x10^{18} dopants/cm^3, the leakage current levels are ~ 10^6 times higher and increase in proportion to the density of trap centers. Since the trap centers are predominately provided by residual implant damage centers, the leakage current for a SDE junction in a halo/well profile is strongly dependent on the success of the implant/anneal process sequence to provide strongly activated, shallow junctions and low defect density regions around the junction.

The increase in junction leakage with increased sub-junction doping and the presence of residual damage has been clearly illustrated for the case of "diffusionless" anneals at 650 C after Ge pre-amorphization implants and shallow B doping [4].

Carrier diffusion

The carrier diffusion contribution to leakage is given by [1,2]:

$$J_{diff} = q\sqrt{\frac{D_p}{\tau_p}}\frac{n_i^2}{N_A} \qquad (6)$$

where τ is the minority carrier lifetime, which follows an Auger recombination mechanism for heavily-doped junctions and D_p is the carrier diffusion coefficient.

The carrier lifetime follows:

$$\tau_p = 1/C_p N_A^2 \qquad (7)$$

where Cp is the Auger recombination coefficient, so the diffusion contribution to leakage is small for the case of highly-doped junctions and

$$J_{diff} = q\sqrt{\frac{D_p}{\tau_p}}\frac{n_i^2}{N_A} \sim q * n_i^2 * (D_p * C_p)^{1/2}. \qquad (8)$$

For biased transistors with metal junction contacts, the additional leakage mechanisms include structure-dependent effects of band-to-band tunneling at the drain junction, thermionic emission from the metal contact and gate-to-channel leakage through the gate dielectric.

Band-to-band tunneling

The band-to-band tunneling current, J_{tun}, is approximated by:

$$J_{tun} = \frac{\pi q^2 m_r V_{rb} E_g E_m}{h^3 E_0} \exp\left(-E_0 / E_m\right) \quad (9)$$

$$W(V_{rb}) = \sqrt{\frac{2\varepsilon_S \varepsilon_0 (V_{bi} - V_{rb})}{q}\left(\frac{N_A + N_D}{N_A N_D}\right)} \quad (10)$$

$$E_m \approx {V_{bi} - V_{rb}}/{W} \quad (11)$$

where E_m is maximum electric field calculated using W, h is a Plank constant, m_r is the effective mass value for the tunneling electron in an indirect band gap material, E_o is a band gap and V_{rb} is applied reverse bias [5]. This form of leakage current is centered on the high-field region of the channel/drain junction and represents a fundamental limit for semiconductor materials, scaled by the band gap energy, E_o.

Thermionic emission

Thermionic emission of carriers from metal contacts through shallow junctions depends on the junction doping level, depth and profile shape, with lower carrier flows for junctions with abrupt, or box-like, profiles [6]. For practical transistors, the effects of thermionc emission are minimized by the deeper junctions used for the source/drain contacts, however this can be a significant issue for measurements with direct contact probes onto shallow extension junctions.

Gate leakage and other effects

Gate-to-channel leakage is, at present, a dominant leakage issue for transistors and the driver for replacement of SiO_2 with high-k dielectrics with EOT values of ~1 nm and less. The thermal stability of these new dielectric materials effects transistor doping by limiting the thermal cycles that can be used for damage annealing and dopant activation.

Additional leakage effects includes surface recombination currents, which are small for heavily-doped, well-activated surface junctions (but could become more important for poorly activated junctions, such as those resulting from unsuccessful ms-timescale anneals), as well as a variety sub-threshold leakage current effects in short-channel CMOS transistors.

3. Leakage currents in RsL measurements

RsL methods measure the junction leakage through analysis of the dependence of the JPV signal on the modulation frequency of the incident LED light beam [3]. The extracted parameter is the amplitude of the diode equation, Io, where the diode current is given by the Shockley equation:

$$J_{diode} = I_o(e^{qV/kT} - 1) \ (A/cm^2). \qquad (12)$$

The recombination current amplitude, I_o, is measured under forward bias in RsL but is also equal to the reverse bias leakage of an "ideal" diode dominated by carrier generation.

In the case of RsL, leakage is measured under very small forward bias, V<<kT/q, created by photo carriers. In this case leakage current includes only contribution of diffusion current J_{diff} and space charge generation current J_{gen} (operating in this case as a recombination current):

$$J_{leakRsL} = J_{diff} + J_{gen} = q\sqrt{\frac{D_p}{\tau_p}}\frac{n_i^2}{N_A} + \sigma \cdot v_{th} n_i N_t \sqrt{\frac{q\varepsilon_S \varepsilon_0 (Na + Nd)Vbi}{2N_A N_D}} \ . \qquad (13)$$

The effect of trap density, N_t, on leakage current for forward (RsL) and reverse (transistors) bias is shown in Fig. 4. In this calculation, the surface junction is heavily doped (so J_{diff} is small), the sub-junction doping levels are high (~$5x10^{18}$ dopants/cm^3) approximating the levels for a halo profile near a SDE junction, and the capture cross-section is σ ~10^{-16} cm^2. For the reverse bias (assumed to be -1V) case, the main additional leakage contribution is assumed to be band-to-band tunneling at a level of J_{tun} ~$5x10^{-4}$ A/cm^2 [5], which sets the leakage current limit for the case of low trap densities.

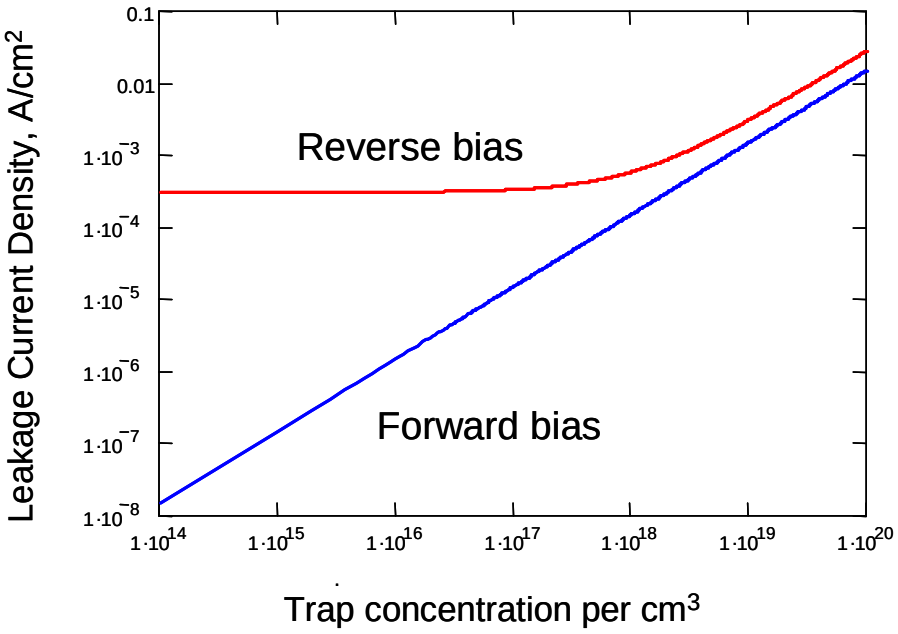

Fig. 4. Leakage current versus trap concentration for reverse bias (-1 V, red curve) and forward bias (+50 mV, blue). The reverse bias curve corresponds to leakage current measurements with diodes and transistors and the weak forward bias case occurs in RsL measurements.

It is important to note that the strong effect of trap (residual damage) density on leakage current shown in Fig. 4 is observed for heavily-doped sub-junction regions similar to the case of SDE junctions formed in halo/well profiles, where the depletion layer thickness, W, is small (~20 nm). For SDE junctions formed in lightly-doped wafers (~ 10 Ohm-cm), the depletion layer is large (~1 um) so the main carrier recombination and generation occurs deep (~ 0.5 um) below the SDE junction and far from the EOR damage layer [3]. In the lightly-doped substrate case, the recombination leakage current will be much lower and show little or no dependence on trap density.

4. Comparison of leakage current measurements for RsL and transistors/diodes

The direct linkage of leakage current measurements between RsL probes of p-n junctions and 3-D structures, such diodes and transistors, is complicated by the number of additional leakage mechanisms in the 3-D structures. The key factor is that RsL measures the components of device leakage which are dependent on process variables, implant and anneal sequences. These are the components of the device leakage which are accessible to optimization without wholesale changes to the transistor structure and materials. Since transistor structures contain additional leakage mechanisms, the recombination leakage measured by RsL is the minimum leakage current levels that characterize a given junction-substrate doping and damage condition.

The effect of the additional leakage current factors, beyond the carrier generation and recombination effects, that are active in diodes and transistors is to limit the dynamic range of leakage current dependence on carrier trap distribution density and location. For the case shown in Fig. 4, where the minimum transistor leakage is limited by a tunneling current of ~$5x10^{-4}$ A/cm^2 [6], the dynamic range of sensitivity to defect density is <10^2. At the high end of the leakage current measurement, the leakage current is limited by factors related to limited thermal processing of shallow junctions; poor dopant activation, thin active and depletion layers and incomplete removal of implant damage.

The RsL method, which is not limited by the materials and structural leakage mechanisms in transistors, has a measurement dynamic range of ~10^5; from ~10^{-7} A/cm^2 for low defect and low sub-junction doping levels to ~$5x10^{-2}$ A/cm^2 for high defect levels in heavily-doped profiles. The wide dynamic range of RsL methods (~10^4 for Rs, ~10^5 for leakage) allows for testing across the full range of CMOS doping processes with a single, well-known parameter for Rs and provides a means of assessing the effects of process variables on defect-driven leakage over a range well beyond the capability of diode testing and with significantly shorter turn around time.

The types of process and recipe-related variables that the RsL can monitor include the effects of dopant dose and depth, damage accumulation, dopant activation and diffusion and local effectiveness of damage reduction during annealing. Damage accumulation during implant depends on a combination of recipe-driven effects (ion type, energy and dose) and process related variables (ion beam current, scan rates and wafer temperature during implant). The recipe related effects can be explored during process development and the process-drive effects are checked for during routine process control sampling.

Doping processing with ms-scale annealing

With the use of ms-scale anneal cycles to reduce dopant diffusion to the low nm level, proportional limitations on Si diffusion create a much higher sensitivity to initial damage distributions following implant and to variations in the complex, multi-component thermal cycles for laser and flash-type annealers. The advantage of the RsL tool is to provide leakage current data on the same time scale and with the same monitor processing costs as sheet resistance monitoring for implant dose, energy and anneal activation. The rapid turn around time for testing, with high-resolution mapping data for Rs and Io available within minutes of the completion of the anneal cycle, is compatible with in-process control activities for critical doping processes.

References:

[1] S.M. Sze, Physics of Semiconductor Devices.
[2] D. K. Schroder, Semiconductor Material and Device Characterization.
[3] V. N. Faifer et al., Proc. of USJ05, to appear in JVST-B, Jan06.
[4] R. Lindsay et al., JVST B22(1), (2004) 306.
[5] P. M. Solomon, et al., IEDM03.
[6] E. C. Jones, N. W. Cheung, JVST B14(1), (1996) 236.